Since January 2020 Elsevier has created a COVID-19 resource centre with free information in English and Mandarin on the novel coronavirus COVID-19. The COVID-19 resource centre is hosted on Elsevier Connect, the company's public news and information website.

Vaccine 27 (2009) 2930–2939

Contents lists available at ScienceDirect

Vaccine

journal homepage: www.elsevier.com/locate/vaccine

In vivo biodistribution of a highly attenuated recombinant vesicular stomatitis virus expressing HIV-1 Gag following intramuscular, intranasal, or intravenous inoculation

J. Erik Johnson*,[1], John W. Coleman[1,2], Narender K. Kalyan, Priscilla Calderon, Kevin J. Wright[2], Jennifer Obregon, Eleanor Ogin-Wilson, Robert J. Natuk, David K. Clarke[3], Stephen A. Udem[3], David Cooper, R. Michael Hendry[4]

Wyeth Vaccines Research, 401 North Middletown Rd, Pearl River, NY 10965, United States

ARTICLE INFO

Article history:
Received 18 December 2008
Received in revised form 3 March 2009
Accepted 4 March 2009
Available online 13 March 2009

Keywords:
Vesicular stomatitis virus
rVSV vector
Biodistribution
Pathogenicity
Attenuation

ABSTRACT

Recombinant vesicular stomatitis viruses (rVSVs) are being developed as potential HIV-1 vaccine candidates. To characterize the in vivo replication and dissemination of rVSV vectors in mice, high doses of a highly attenuated vector expressing HIV-1 Gag, $rVSV_{IN}$-N4CT9-Gag1, and a prototypic reference virus, $rVSV_{IN}$-HIVGag5, were delivered intramuscularly (IM), intranasally (IN), or intravenously (IV). We used quantitative, real-time RT-PCR (Q-PCR) and standard plaque assays to measure the temporal dissemination of these viruses to various tissues. Following IM inoculation, both viruses were detected primarily at the injection site as well as in draining lymph nodes; neither virus induced significant weight loss, pathologic signs, or evidence of neuroinvasion. In contrast, following IN inoculation, the prototypic virus was detected in all tissues tested and caused significant weight loss leading to death. IN administration of $rVSV_{IN}$-N4CT9-Gag1 resulted in detection in numerous tissues (brain, lung, nasal turbinates, and lymph nodes) albeit in significantly reduced levels, which caused little or no weight loss nor any mortality. Following IV inoculation, both prototypic and attenuated viruses were detected by Q-PCR in all tissues tested. In contrast to the prototype, $rVSV_{IN}$-N4CT9-Gag1 viral loads were significantly lower in all organs tested, and no infectious virus was detected in the brain following IV inoculation, despite the presence of viral RNA. These studies demonstrated significant differences in the biodistribution patterns of and the associated pathogenicity engendered by the prototypic and attenuated vectors in a highly susceptible host.

1. Introduction

Vesicular stomatitis virus (VSV) is a prototypic virus of the Rhabdoviridae family, belonging to the order Mononegavirales, which encompasses single stranded, nonsegmented, negative-sense RNA viruses with highly conserved gene order [1]. The two most common serotypes of VSV in the western hemisphere are designated as Indiana (VSV_{IN}) and New Jersey (VSV_{NJ}). In nature, VSV infects livestock causing a self-limiting disease. Although naturally occurring human infections with VSV are rare, VSV infections have been reported for individuals directly exposed to infected livestock, within laboratory environments, and living within endemic regions [2–11]. VSV infection of humans is typically either asymptomatic or causes a mild influenza-like illness [6]. Among small mammals, mice are readily infected experimentally via a variety of inoculation routes and thus have served as a tractable model for immunogenicity, pathogenicity, neurotropism and neurovirulence studies [12–20].

VSV has shown promise as a vaccine vector for a wide variety of human pathogens including HIV, papilloma virus, respiratory syncytial virus, SARS coronavirus, Ebola virus, Marburg virus, herpes simplex virus, Lassa fever virus, influenza virus [for review, see Ref. [21]], and hepatitis C virus [22]. Most of these studies were conducted with prototypic, recombinant VSV (rVSV) vectors that were derived from tissue culture-passaged, wild type (wt) VSV strains, which were shown to be somewhat attenuated when compared to the wt VSV [23]. More recently, in a non-human primate model for neurovirulence, we showed that the prototypic rVSV vectors caused a significant level of neuropathology following direct intrathalamic

* Corresponding author. Tel.: +1 845 602 2101; fax: +1 845 602 4977.
E-mail address: johnsoe1@wyeth.com (J. Erik Johnson).
[1] These authors contributed equally to this work.
[2] Current address: IAVI, 140 58th Street, Brooklyn, NY 11220, United States.
[3] Current address: Profectus Biosciences, Inc., 520 White Plains Road, Suite 500, Tarrytown, NY 10591, United States.
[4] Current address: CDC, 1600 Clifton Road, Atlanta, GA 30329, United States.

0264-410X/$ – see front matter © 2009 Elsevier Ltd. All rights reserved.
doi:10.1016/j.vaccine.2009.03.006

injection, albeit at reduced levels compared to the wild type virus [24]. These observations led to the conclusion that the prototypic rVSV vectors required further attenuation and preclinical analysis prior to clinical evaluation.

In the process of generating rVSVs with reduced vector pathogenicity, we developed a highly attenuated rVSV vector expressing the HIV-1 Gag gene, $rVSV_{IN}$-N4CT9-Gag1, which was made by combining three attenuating approaches: insertion of HIV-1 Gag gene in the first position of the genome, shuffling of VSV N gene to the fourth position (N4) and use of a VSV G with its cytoplasmic tail truncated from 29 to 9 amino acids (CT9) [25–27]. Because there is an established gradient of transcription for VSV in which genes proximal to the single 3′ genomic promoter are expressed to the highest levels with a decrease in transcription for each gene as its distance from this promoter increases [28–33], we anticipated high levels of Gag expression, a concomitant reduction in VSV N expression, and a high degree of attenuation for the $rVSV_{IN}$-N4CT9-Gag1 vector as compared to the prototypic rVSV. Indeed, the in vivo attenuation of $rVSV_{IN}$-N4CT9-Gag1 was characterized by a dramatic rise in the mouse LD_{50} following intracranial (IC) inoculation [34]. However, this vector retained the ability to grow in vitro to high titers, and was capable of inducing immune responses in mice and macaques that were comparable to those obtained with the prototypic vector, rVSV-HIVGag5 ([34], and unpublished observations).

An important aspect of characterizing a potential vaccine vector is to determine its pathogenicity and tissue distribution following in vivo administration. Notably, there is no experience with administration of rVSV vectors to humans, and when human infection with VSV does occur, it is not known which tissues are affected nor how the infection spreads. Therefore, we assessed the in vivo distribution and replication of prototypic ($rVSV_{IN}$-HIVGag5) and attenuated ($rVSV_{IN}$-N4CT9-Gag1) rVSV vectors in mice following three different routes of administration: intramuscular (IM), intranasal (IN), and intravenous (IV). The IM and IN routes were chosen because they have been considered for clinical evaluation. Furthermore, we tested the IV route to evaluate the effects of widespread dissemination of the viruses [35]. As an increased stringency parameter, we used a high dose of rVSV vectors in these studies, 10^8 plaque forming units (PFU) per animal.

2. Materials and methods

2.1. Mice

All animal care and procedures conformed to Institutional Animal Care and Use Committee guidelines. The facilities are fully accredited by the American Association for Accreditation of Laboratory Animal Care. Six- to seven-week old, inbred female BALB/c mice were obtained from Taconic Farms (Germantown, NY) and were acclimated for 1 week prior to inoculation. Transponders (BioMedic Data Systems Inc., Rockville, MD) used to identify mice and to aid in recording body weights and temperatures were inserted subcutaneously into the backs of mice as per the manufacturer's instructions. During the course of these studies mice were closely monitored for signs of neurological disease such as paralysis or seizures. Any mice that exhibited signs of physical disability such as inactivity to stimulation, seizures, or complete paralysis were euthanized.

2.2. Viruses

The $rVSV_{IN}$-HIVGag5 and the $rVSV_{IN}$-N4CT9-Gag1 viruses have been previously described [24,34]. To prepare viral stocks for inoculating mice, baby hamster kidney cells (BHKs) were infected with each virus at a multiplicity of infection (MOI) between 0.1 and 1.0. The $rVSV_{IN}$-HIVGag5 virus was harvested after 24 h at 37 °C, and the $rVSV_{IN}$-N4CT9-Gag1 virus was harvested after 48 h at 32 °C. The harvested culture media was first subjected to a low-speed centrifugation (1500 rpm, 5 min, 4 °C in a Beckman GS-6KR Refrigerated Centrifuge), and the supernatants were layered onto 10% sucrose cushions. Following ultracentrifugation (28,000 rpm, 80 min, 4 °C in a Beckman SW28 rotor), media and sucrose was discarded and viral pellets were resuspended in phosphate buffered saline (PBS, Mediatech). Aliquots of reconstituted viruses were frozen in dry ice/ethanol baths and stored frozen at −80 °C. To determine potency of virus stocks, an aliquot of each was thawed and titered on Vero cells in duplicate according to the procedure below.

2.3. Inoculations and clinical observations

Immediately prior to animal inoculations, frozen virus stocks were rapidly thawed at 37 °C for 3–5 min, briefly mixed in a vortexer, and placed immediately on ice. Based on the concentration, each virus was diluted in PBS to a concentration of 10^8 PFU/dose. PBS was used as a negative control for each group of mice. For IM and IN inoculations, mice were anesthetized with an IP injection of Ketamine (105 mg/kg) and Xylazine (10 mg/kg) diluted with sterile saline. For IM inoculations, each mouse was given one 50-μL injection in the right calf muscle. For IN inoculations, each mouse was given two 5-μL doses in the nose with a pause between inoculations to ensure proper uptake in nasal passages. For IV inoculations, mice were carefully warmed with a heat lamp and each mouse was given one 200-μL injection into a lateral tail vein. The health status of all mice was recorded for the study duration; in the day 24 groups of mice, weights and body temperatures were recorded daily for 2 weeks. Mice becoming bilaterally paralyzed or showing signs of distress or severe illness were euthanized and recorded as succumbing to VSV disease.

2.4. Tissue harvest and preparation

Tissues were harvested after transcardial perfusion with saline of the animal to remove any blood-associated VSV from the harvested organs (perfusion was not performed on mice receiving VSV IM, as previous studies showed that there is no VSV viremia following inoculation by this route). Mice were either euthanized by inhalation of CO_2 (for IM study) or anesthetized as described above and perfused (for IV and IN studies). In the latter case, death was achieved by the exsanguination caused by the perfusion. For perfusion, animals were placed in dorsal recumbency, the abdomen was wet with alcohol, and an incision was then made at the abdominal midline. The thoracic cavity was opened exposing the heart and lungs. A 20–21 gauge needle was then attached to a fluid bag containing PBS with an IV set. The needle was put into the apex of the left ventricle. The fluid line was then opened fully. The right auricle was then snipped. Sufficient fluid (maximum 100 mL) was then allowed to pump through the vasculature to evacuate all blood from the animal. The following organs were harvested from mice and tested for the presence of VSV RNA or virus: brain, liver, lung, kidney, spleen, muscle (corresponding to injection site for IM route, in the IM and IV studies only), nasal turbinates (IN studies only) and draining lymph nodes (popliteal, inguinal, and iliac for IM; and cervical for IN). Blood was also collected at the time of organ harvest, prior to perfusion. Each piece of tissue was weighed, suspended in 4 °C phosphate-buffered saline (PBS)/sucrose phosphate buffer with glutamine (SPBG, 0.2 M sucrose, 7.0 mM K_2HPO_4, 3.8 mM KH_2PO_4, 5.0 mM glutamic acid) to 10% weight/volume (w/v), and homogenized using an Omni Tip™ Tissue Homogenizing Kit with autoclavable probes. Lymph nodes and nasal turbinates were resuspended directly in 2.0 mL PBS/SPBG, producing an approximate 10% (w/v) suspension. For determination of viral loads, 140 μL aliquots

were removed and stored at −70 °C for RNA extraction and virus titration.

2.5. Quantitative real-time RT-PCR

Viral nucleic acid was extracted from homogenized tissues using the RNeasy Mini kit (Qiagen, Valencia, CA) and was reverse transcribed into cDNA using methods previously described [36]. Briefly, detection of viral genomic RNA (negative sense) was done in a 20-μL reaction mix containing total RNA from tissue samples (5.0 μL or 0.5 μg), VSV N and the large ribosomal protein L15 housekeeping gene (RPLO) forward primers, and reagents from the Sensiscript Reverse Transcriptase kit (Qiagen). To detect mRNA transcripts, 10 μM of the anchored oligo-dT primer was substituted for the VSV N specific-forward primer. Otherwise, the reagents and the conditions for the reverse transcription step remained as described. Primer and probe sets for detecting RNA encoding VSV N and HIV Gag and the primer nucleotide sequence for the anchored oligo-dT primer have been previously described [36]. The primer-probe set RPLO was selected using the Primer Express software version 2.0 (Applied Biosystems, Foster, CA) and contained the following sequences: forward primer, 5′-GCCAGCTCAGAACACTGGTCTAG-3′ (anneals between residues 443 and 465); reverse primer, 5′-ATGCCCAAAGCCTGGAAGA-3′ (anneals between residues 484 and 502); TaqMan probe, 5′-CCGAGAAGACCTCC-3′ (anneals between residues 469 and 482). The duplex quantitative real-time PCR to detect genomic RNA was carried out using the QuantiTect Multiplex PCR Kit (Qiagen). A 30-μL PCR reaction containing 5 μL of each 10-fold dilution of the VSV N, HIV Gag, and RPLO cDNA used to generate standard curves or 5 μL of cDNA from tissue samples, 15 μL of 2× QuantiTect Multiplex PCR Master Mix, 400 nM each of the forward and reverse primers for VSV N and RPLO, and 200 nM of each probe. For the duplex assay to detect mRNA from cDNA, the reaction mix remained the same except HIV Gag and RPLO forward and reverse primers and probes were used. In order to distinguish the amplicons, the probes for VSV-N were labeled with FAM (6-carboxyfluorescein), HIV-Gag with VIC (6-carboxyrhodamine 6G), and RPLO with NED. Amplification and detection were performed with an ABI Prism 7500 Fast Real-Time PCR System using the following conditions: 15 min at 95 °C to activate the HotStar Taq DNA polymerase, followed by 40 cycles of 60 s at 94 °C and 90 s at 60 °C. All samples were tested in duplicate. For calculating group means, the detection limit was used for any sample that was below the limit of detection of the assay (5×10^3 copies/10 mg of tissue or 4×10^4 copies/mL of blood).

2.6. Virus titration

Briefly, the titer of virus was determined by performing 10-fold serial dilutions of samples in DMEM supplemented with 2% FBS. One-tenth the volume of each serial dilution (0.1 mL) was used to infect confluent Vero cell monolayers in 6-well plates (each sample infected in duplicate wells). After adding 0.4 mL of DMEM/2% FBS per well, infected cells were incubated at room temperature (RT) for 15 min followed by 37 °C for 30 min (in 5% CO_2 incubator). The inoculum was removed from each well and replaced with 3.0 mL of 1% Sea Plaque agarose (Cambrex) in DMEM/2% FBS overlay. The plates were incubated in a 32 or 37 °C incubator until plaque formation (24–48 h). Agarose plugs were carefully removed with a small spatula, and the monolayers were fixed with 1:1 methanol: acetone mixture (2.0 mL per well) at RT for 30 min. After washing with PBS, 1.5 mL of blocking solution (5% milk in 0.1% Tween-20 Tris Buffered Saline [TTBS]) was added to each well and incubated at RT for 30–60 min. Following PBS wash, the monolayers were incubated at RT for 1 h with 1.0 mL per well of primary antibodies (1:1 mixture if mAbs I-1 and I-14 [37] diluted 1:2000 in TTBS). Monolayers were then washed with PBS and incubated at RT for 30–60 min with secondary antibody (horseradish peroxidase-conjugated goat anti-mouse IgG [Biorad] diluted 1:2000 in TTBS). Following PBS wash, the monolayers were incubated at RT for 5–10 min with 1.0 mL per well of DAB substrate (one 3,3ï-Diaminobenzidine Tablet [Sigma] in 20 mL PBS and 7 μL H_2O_2). After counting the stained plaques, the virus titer was calculated as mean PFU/10 mg of homogenized tissue or PFU/mL of blood. For calculating group means, the detection limit was used for any sample that was below the limit of detection of the assay (0.5 PFU/10 mg of tissue or 50 PFU/mL of blood).

2.7. Statistical analyses

Data are expressed as mean ± SEM of five mice per test group. Where appropriate, statistical comparisons were conducted on log-transformed data using two-tailed unpaired *t* tests. In cases where all observations in one of the groups were below the limits of detection, Fisher's exact test was used. A value of $p < 0.05$ was considered statistically significant and the degree of significance is represented in figures by: $^{*}p < 0.05$; $^{**}p < 0.001$; $^{***}p < 0.0001$.

2.8. Histopathology

Whole brains were fixed in 10% formalin immediately following necropsy. For each mouse, transverse, H&E-stained tissue sections of the olfactory lobes (OL), the cerebrum at the level of the corpus callosum, the cerebrum at the level of the optic chiasm, and the cerebellum with medulla oblongata at the level of the paraflocculus were examined by a board certified veterinary pathologist. Each section was evaluated for the following diagnostic criteria: inflammation, perivascular (cuffing); inflammation/degeneration, neuronal/neurophil (gliosis); inflammation/degeneration, ventricular/periventricular; inflammation, meninges; degeneration, axonal or myelin; vacuolation, neurophil.

For each of the diagnostic criteria, a subjective severity score was assigned, using a scale where: 0 = normal, change not present; 1 = change present, minimal severity; 2 = change present, mild severity; 3 = change present, moderate severity; 4 = change, present, marked severity; 5 = change present, severe.

3. Results

Previous studies have shown that a highly attenuated vector, $rVSV_{IN}$-N4CT9-Gag1 (hereafter referred to as N4CT9-Gag1), had greatly reduced neurovirulence yet retained potent immunogenicity in mice compared to the prototypic vector, $rVSV_{IN}$-HIVGag5, hereafter referred to as Gag5 [34]. To better understand virus dissemination following vaccination, we performed a series of studies comparing the tissue distribution of these two vectors in mice, following high dose (10^8 PFU) administration by the IM, IN, or IV routes. The initial study design included tissue harvests on days 0 (4 h post-inoculation), 1, 2, 4, and 8 post-inoculation for viral load assessment; however, because of persistent viral RNA in some tissues at day 8 in the IM study, additional later time points were collected in both the IN and IV studies.

3.1. Pathologic parameters following IM inoculations

Mice were inoculated by the IM route with Gag5, N4CT9-Gag1, or PBS as a control and monitored clinically for 2 weeks. Mice in the Gag5 group lost an average of 5% of their body weight on day 1 after inoculation and returned to normal weight by day 3, after which their weights matched the trend observed for the PBS control mice (Fig. 1A). There were no significant differences in body temperatures between the Gag5 group and the PBS group (data not shown), nor any clinical signs such as matted fur, paralysis, or death

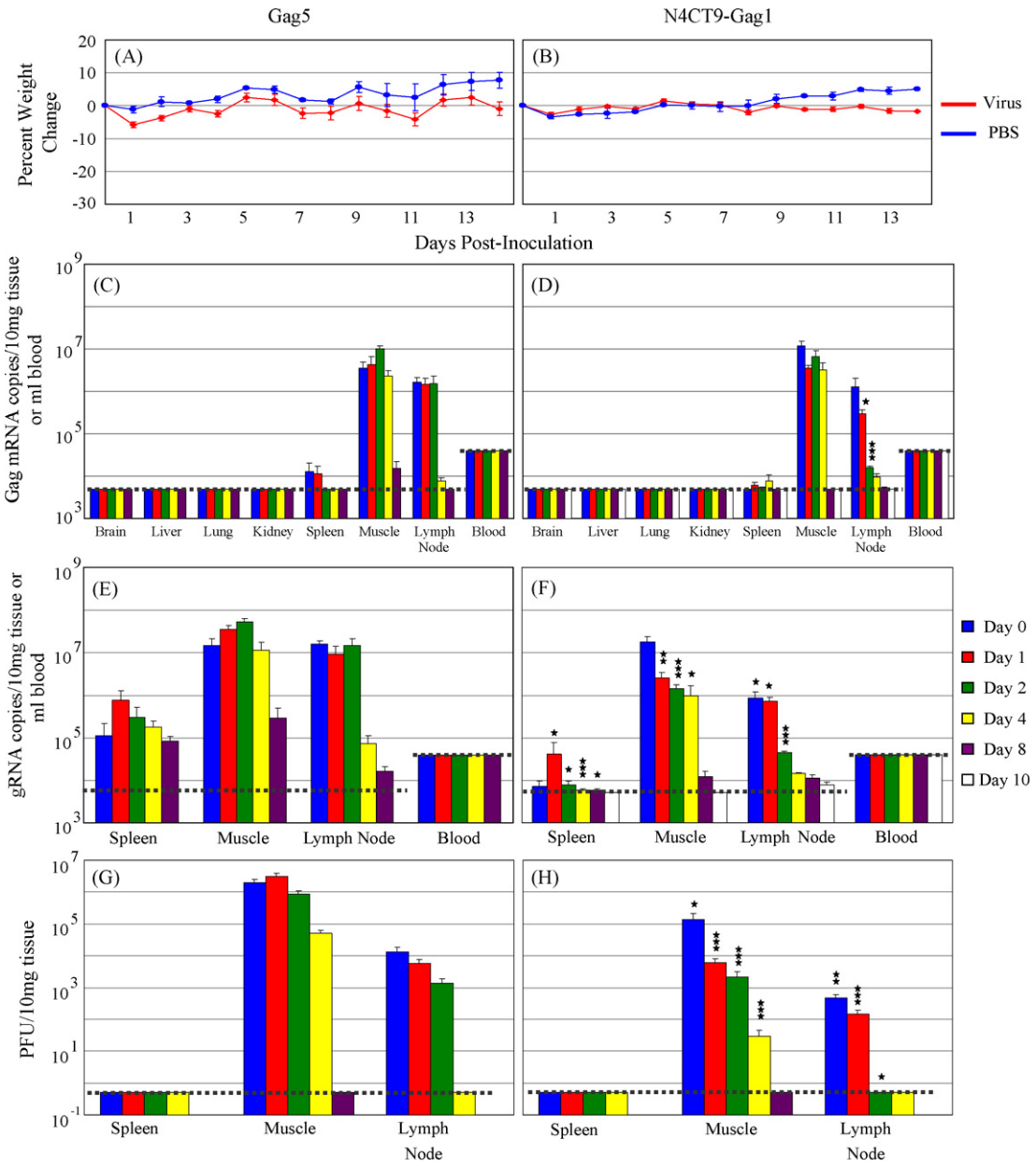

Fig. 1. Mouse body weights and viral loads following IM inoculation. (A and B) Average body weights expressed as the percent change from day 0 weights versus days post-inoculation. (C and D) Average Gag mRNA copies per 10 mg of the indicated tissue or per mL of blood as determined by Q-PCR. (E and F) Average gRNA copies per 10 mg of the indicated tissues or per mL of blood as determined by Q-PCR. (G and H) Average infectious virus in plaque forming units (PFU) per 10 mg of tissue or per mL of blood as determined by standard plaque assay. (A), (C), (E), and (G): mice inoculated with $rVSV_{IN}$-HIVGag5. (B), (D), (F), and (H): mice inoculated with $rVSV_{IN}$-N4CT9-Gag1. Dotted lines indicate limits of detection of the assays. Limit of detection for Q-PCR = 5×10^3 copies/10 mg of tissue or 4×10^4 copies/mL of blood. Limit of detection of the plaque assay = 0.5 PFU/10 mg of tissue or 50 PFU/mL of blood. Bars at each time point indicate standard error. For comparison of $rVSV_{IN}$-HIVGag5 to $rVSV_{IN}$-N4CT9-Gag1, $^{*}p < 0.05$; $^{**}p < 0.001$; $^{***}p < 0.0001$.

Table 1
Clinical signs of disease in mice following inoculation.

Virus	Route	Number of mice immunized	Clinical Observation			
			Matted Fur	Paralysis	Euthanized	Found Dead
$rVSV_{IN}$-HIVGag5	IM	35	0 (0%)	0 (0%)	0 (0%)	0 (0%)
	IV	50	50 (100%)	2 (4%)	2 (4%)	0 (0%)
	IN	90	90 (100%)	8 (8.9%)	8 (8.9%)	6 (6.7%)
$rVSV_{IN}$-N4CT9-Gag1	IM	35	0 (0%)	0 (0%)	0 (0%)	0 (0%)
	IV	50	0 (0%)	0 (0%)	0 (0%)	0 (0%)
	IN	50	0 (0%)	0 (0%)	0 (0%)	0 (0%)

(Table 1). Following IM inoculation with N4CT9-Gag1, the average body weights (Fig. 1B) and temperatures (data not shown) of the mice showed no differences when compared to the PBS control group, and these mice appeared clinically normal (Table 1).

3.2. Viral loads following IM inoculations

Following IM administration, the Gag5 virus was detected at the injection site, in draining lymph nodes, as well as in the spleen (Fig. 1C, E, and G). In the muscle, high levels of mRNA, gRNA, and infectious virus were measured on days 0–4, with detectable levels of Gag mRNA and gRNA persisting through day 8. Similarly, Gag mRNA, gRNA, and infectious virus were detected at high levels in lymph nodes on days 0–2, with Gag mRNA and infectious virus reaching undetectable levels by day 8 or 4, respectively. In spleens, low levels of Gag mRNA were only detected on days 0 and 1; however, gRNA copies persisted through day 8.

In the N4CT9-Gag1 group, viral loads were similarly detected in muscle, lymph nodes, and spleen tissue from mice following IM injection (Fig. 1D, F, and H). Because the viral RNA levels had not reached undetectable levels by day 8 in the Gag5 group, we harvested tissues from N4CT9-Gag1-inoculated mice at an additional time point, day 10. Again, the highest viral loads were observed in muscle tissue, where Gag mRNA, gRNA, and infectious virus levels peaked on day 0, remained relatively high through day 4, and reached undetectable levels by day 8 (Gag mRNA and infectious virus) or day 10 (gRNA). In muscle tissue, the gRNA and infectious virus levels in the N4CT9-Gag1 group were significantly lower than in the Gag5 group at most time points. In the lymph nodes, viral loads peaked on day 0 and decreased to undetectable by day 2 (infectious virus) or day 8 (Gag mRNA); low levels of gRNA persisted through day 10. Viral loads in the lymph nodes were significantly lower in the N4CT9-Gag1 group than in the Gag 5 group at several time points. Finally, the gRNA levels in the spleen were significantly lower in the N4CT9-Gag1 group than in the Gag5 group at nearly all time points. As was observed in the Gag5 group, no infectious N4CT9-Gag1 was detected in spleen tissues on days 0–4.

3.3. Pathologic parameters following IN inoculations

Mice inoculated by the IN route with either Gag5, N4CT9-Gag1, or PBS as a control were monitored clinically for 2 weeks. Mice in the Gag5 group lost weight steadily until days 5–6, at which time they had lost an average of 25% of their initial body weights (Fig. 2A); all of the mice appeared ill (Table 1). Mice that did not die nor required euthanasia began to gain weight following day 7, but never recovered to the day 0 levels. Although the average body temperatures in these mice were similar to the PBS control group throughout the study (data not shown), 100% of these mice in the Gag5 group had matted fur, 9% developed paralysis, and a total of 16% died by euthanasia or from disease (Table 1). In contrast, mice in the N4CT9-Gag1 group did not exhibit signs of weight loss until day 4, when they lost an average of 5% of their original body weights (Fig. 2B). The average body weights then gradually returned to initial levels by day 8. The average body temperatures were equivalent to the PBS control group (data not shown), and there were no additional clinical abnormalities (Table 1).

3.4. Viral loads following IN inoculations

In mice inoculated with Gag5 by the IN route, viral mRNA and gRNA were detected in all tissues tested (Fig. 2E and C, respectively). As in the IM study, Gag mRNA, gRNA, and infectious virus were detected at the highest levels at the site of inoculation, in this case the nasal turbinates. While overall viral loads varied among the different tissues, the Gag mRNA copies, gRNA copies, and titers of infectious virus displayed similar kinetics in each tissue type; furthermore, Gag mRNA and gRNA copies were nearly equivalent in most tissues. Based on the tissue distribution at day 0, the inoculum appeared to be contained in the nasal turbinates and lungs; however, a small number of viral genomes (but no Gag mRNA) were detected in the brain tissue of mice on day 0, which presumably corresponded to input virus. Gag mRNA and/or gRNA persisted the longest in brain (day 17), nasal turbinates and lymph nodes (both day 34, with one mouse for each tissue having Gag mRNA just above the detection limit at day 41). Infectious virus was cleared from all tissues by day 4 or 8, except for brain tissue, where it was cleared by day 10.

Mice that were inoculated with N4CT9-Gag1 by the IN route had detectable Gag mRNA, gRNA, and/or infectious virus in the following tissues: brain, lung, nasal turbinates, and lymph nodes (Fig. 2D, F, and H). Only one mouse had both Gag mRNA and gRNA copies just above the detection limit on day 2 in the spleen. In addition, one mouse had detectable gRNA in the liver at day 0 (Fig. 3F). As in the Gag5 group, N4CT9-Gag1 Gag mRNA and gRNA persisted the longest in brain (day 17), nasal turbinates (day 17, with one mouse having gRNA just above the detection limit at day 31), and lymph nodes (day 31). Infectious virus was cleared from the lung by day 1 and the lymph nodes by day 4, but did not reach undetectable levels in nasal turbinates or brain until day 8. In most tissues at most time points, the N4CT9-Gag1 viral loads were significantly lower than those of the Gag5 virus. Overall, there were more significant differences in gRNA levels (Fig. 2F) for these two viruses than were observed for Gag mRNA. Finally, infectious virus was significantly lower in mice treated with N4CT9-Gag1 when compared to the Gag5 group in all tissues tested, excluding blood, where N4CT9-Gag1 was undetectable at all time points tested. Of particular note in the N4CT9-Gag1 group, peak infectious titers and gRNA levels detected in brain tissues (day 2) were 100-fold and 500-fold lower, respectively, than the Gag5 group.

3.5. Histopathology following IN inoculations

Fixed brains were sectioned, examined, and scored as described in Materials and Methods (Table 2). One mouse inoculated with Gag5 virus by the IN route exhibited mild inflammation with minimal neurophil vacuolation at day 8 in two sections examined. At day 24, focal, minimal perivascular inflammation was present in one section examined from one of six mice. Microscopic changes were not observed in any other sections examined from Gag5-inoculated mice or in any sections from either the N4CT9-Gag1 or PBS groups at days 8 or 24.

3.6. Pathologic parameters following IV inoculations

High dose IV inoculations of mice with Gag5, N4CT9-Gag1, or PBS as a control were included as a stringent means of analyzing vector-associated pathogenicity and widespread dissemination. In the IV Gag5 group, mice lost 10% of their initial body weights on days 1–2 and slowly regained weight over the course of the study (Fig. 3A). Although there were no differences in body temperatures compared to the PBS control group (data not shown), 100% of these mice had matted fur and 4% became paralyzed, requiring euthanasia (Table 1). Mice inoculated with N4CT9-Gag1 by the IV route lost 5% of their body weight on day 1, but quickly returned to normal weights by day 2 (Fig. 3B). Again, there were no differences in body temperatures compared to the PBS group (data not shown). Additionally, no clinical signs were observed in any of the mice (Table 1).

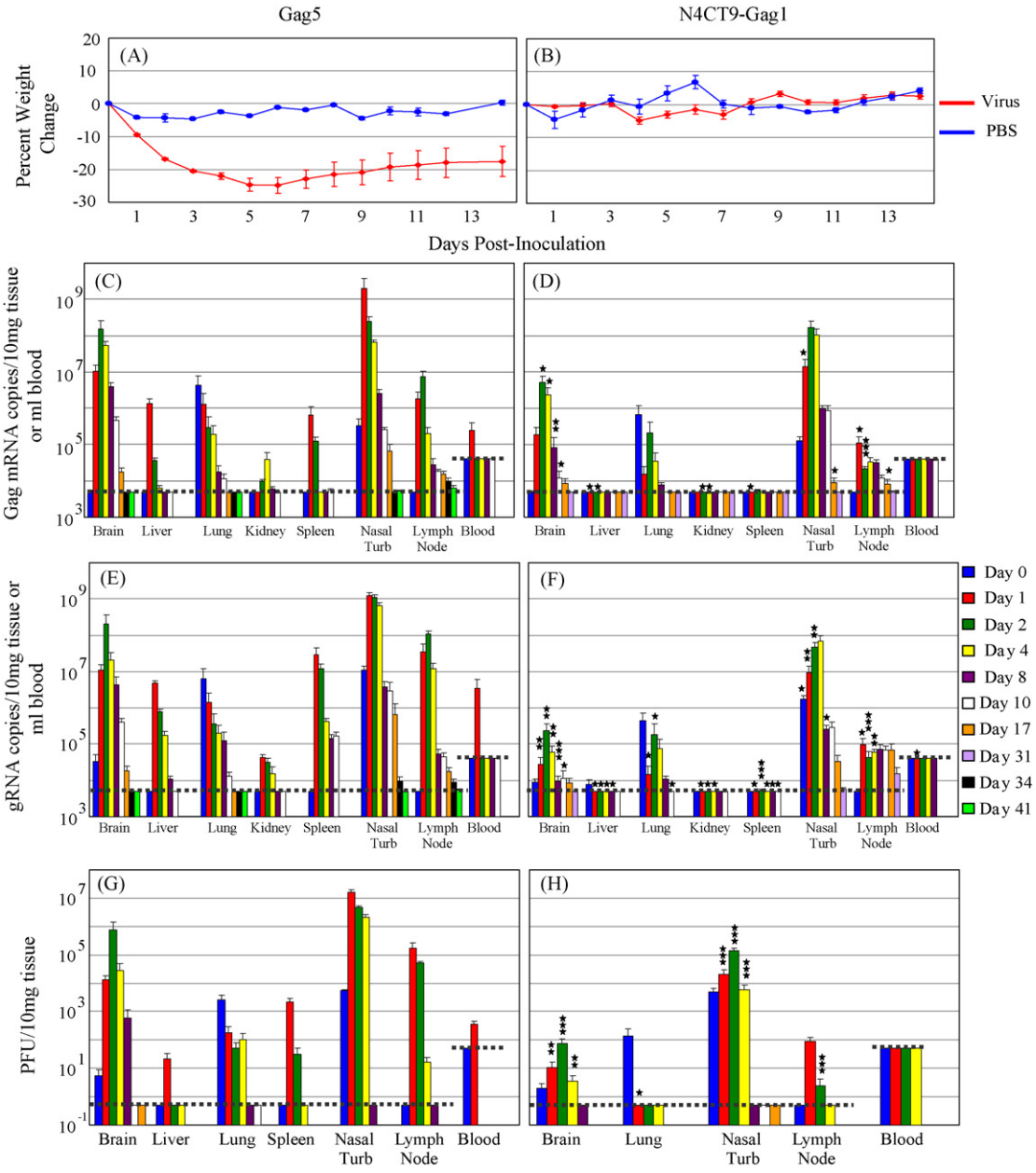

Fig. 2. Mouse body weights and viral loads following IN inoculation. (A and B) Average body weights expressed as the percent change from day 0 weights versus days post-inoculation. (C and D) Average Gag mRNA copies per 10 mg of the indicated tissue or per mL of blood as determined by Q-PCR. (E and F) Average gRNA copies per 10 mg of the indicated tissues or per mL of blood as determined by Q-PCR. (G and H) Average infectious virus in plaque forming units (PFU) per 10 mg of tissue or per mL of blood as determined by standard plaque assay. (A), (C), (E), and (G): mice inoculated with $rVSV_{IN}$-HIVGag5. (B), (D), (F), and (H): mice inoculated with $rVSV_{IN}$-N4CT9-Gag1. Dotted lines indicate limits of detection of the assays. Limit of detection for Q-PCR = 5×10^3 copies/10 mg of tissue or 4×10^4 copies/mL of blood. Limit of detection of the plaque assay = 0.5 PFU/10 mg of tissue or 50 PFU/mL of blood. Bars at each time point indicate standard error. For comparison of $rVSV_{IN}$-HIVGag5 to $rVSV_{IN}$-N4CT9-Gag1, $^{*}p < 0.05$; $^{**}p < 0.001$; $^{***}p < 0.0001$.

3.7. *Viral loads following IV inoculations*

Following IV inoculation with Gag5, virus was detected in all tissues tested (Fig. 3C, E, and G), particularly in the Q-PCR assay. In the blood, viral loads peaked on days 0–1 and were cleared between days 2 and 4. The highest viral loads were detected in the spleen, in which virus was cleared by day 4 but gRNA remained detectable through day 10. In liver, lung, kidney, and muscle, viral RNA peaked between days 0–2 and was at or near the detection limit by day 8; furthermore, infectious virus was either undetectable in these tissues (lung and kidney) or was cleared by day 4 (liver and muscle). Viral loads in the lymph nodes were found to be highest on days 0–2 and persisted through day 4 (infectious virus), day 8 (Gag mRNA), or day 17 (gRNA), which was the last time point taken for this route. Finally, viral loads peaked in the brain at later time points than other tissues, and while infectious virus was cleared by day 8, Gag mRNA persisted through day 10 and gRNA persisted through day 17 in two out of five mice.

Viral loads were similarly detected in all tissues tested in the IV N4CT9-Gag1 group (Fig. 3D, F, and H). In this group, the highest viral loads were also observed in the spleen, in which infectious virus was cleared by day 4 and viral RNA, particularly genomic, persisted through day 10. In liver, lung, kidney, and muscle, viral RNA was detectable only on days 0–2 (with low levels of gRNA still detectable in liver tissue on day 4), and infectious virus was undetectable in all of these tissues except muscle (days 0–1). In the lymph node,

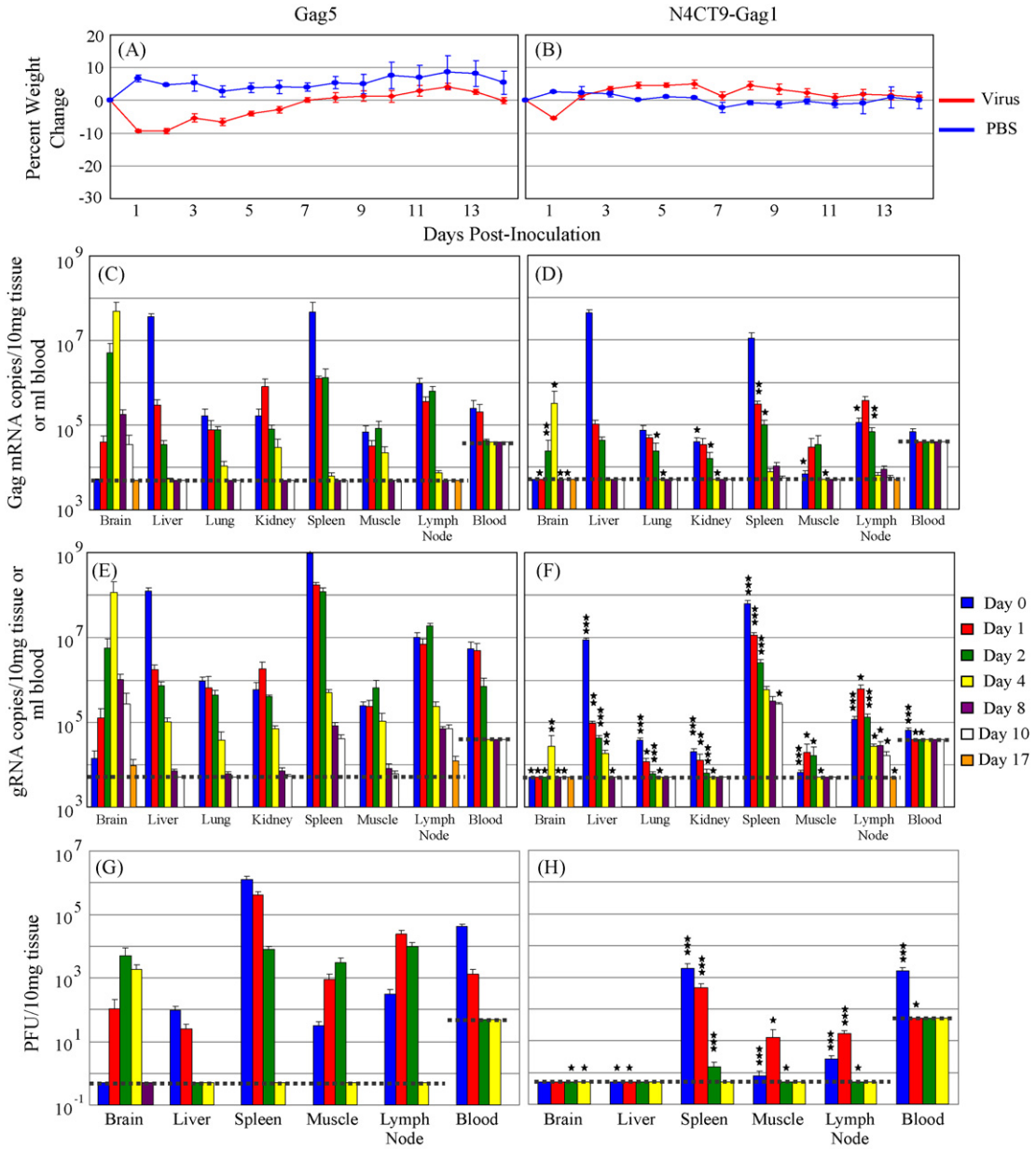

Fig. 3. Mouse body weights and viral loads following IV inoculation. (A and B) Average body weights expressed as the percent change from day 0 weights versus days post-inoculation. (C and D) Average Gag mRNA copies per 10 mg of the indicated tissue or per mL of blood as determined by Q-PCR. (E and F) Average gRNA copies per 10 mg of the indicated tissues or per mL of blood as determined by Q-PCR. (G and H) Average infectious virus in plaque forming units (PFU) per 10 mg of tissue or per mL of blood as determined by standard plaque assay. (A), (C), (E), and (G): mice inoculated with $rVSV_{IN}$-HIVGag5. (B), (D), (F), and (H): mice inoculated with $rVSV_{IN}$-N4CT9-Gag1. Dotted lines indicate limits of detection of the assays. Limit of detection for Q-PCR = 5×10^3 copies/10 mg of tissue or 4×10^4 copies/mL of blood. Limit of detection of the plaque assay = 0.5 PFU/10 mg of tissue or 50 PFU/mL of blood. Bars at each time point indicate standard error. For comparison of $rVSV_{IN}$-HIVGag5 to $rVSV_{IN}$-N4CT9-Gag1, $^{*}p < 0.05$; $^{**}p < 0.001$; $^{***}p < 0.0001$.

Table 2
Brain histopathology results.

Virus	Route[a]	Day	No. with lesions/no. in group[b]	Observations[c]
$rVSV_{IN}$-HIVGag5	IN	8	1/5	Mild inflammation and minimal neurophil vacuolation
		24	1/6	Minimal perivascular inflammation
	IV	8	3/5	Minimal to mild multifocal inflammation
		24	0/5	
$rVSV_{IN}$-N4CT9-Gag1	IN	8	0/5	
		24	0/5	
	IV	8	0/5	
		24	0/5	

[a] The IM samples were not tested because there were no measurable viral loads in the brain tissue samples at any time point post-inoculation.
[b] Number of animals that had at least one lesion in one brain section compared to the number of animals in that group.
[c] All animals in PBS groups were negative at days 8 and 24 in both the IN and IV routes.

while infectious virus was cleared by day 2, viral RNA remained detectable through day 10 (Fig. 3H). In the brain, viral RNA peaked on day 4 and was undetectable by day 8. As in the IN study, the gRNA levels measured in the N4CT9-Gag1 group were significantly lower than in the Gag5 group at more time points than the Gag mRNA levels, although the latter still demonstrated significant differences between these two groups (Fig. 3D and F). Additionally, in each tissue and time point that infectious N4CT9-Gag1 virus was detected, the levels were significantly lower than the Gag5 virus (Fig. 3H) in the corresponding tissues.

3.8. Histopathology following IV inoculations

For mice inoculated IV with Gag5 virus, minimal to mild multifocal, nonsuppurative inflammation was observed in three of five mice in the day 8 samples, and no changes were observed in the brains of day 24 mice (Table 2). No changes were present in the brains of the N4CT9-Gag1 groups or the PBS control mice at either day 8 or 24.

4. Discussion

While mice are not considered a natural host for VSV, they have been used as an animal model for studying VSV pathogenesis for over 70 years [38]. The exquisite sensitivity of mice to VSV infection has proven them as a valuable research tool for assessing virulence of wild type and attenuated strains of VSV [12–20]. While the neurovirulence associated with VSV infection in mice has been well studied, there has not been much advancement in the understanding of the biodistribution of VSV in mice since the pioneering work of Sabin and Olitsky in the 1930s [39–43]. Presently, we used highly sensitive Q-PCR assays to determine that for both the highly attenuated N4CT9-Gag1 and prototypic Gag5 viruses, infection was limited to the inoculation site and draining lymphoid organs following IM inoculation, while more widespread infection was detected when viruses were inoculated via the IN or IV route.

Recombinant VSV vectors are currently being developed as vaccine vectors for HIV and other pathogens, and as with any live viral vector, they must be sufficiently attenuated to be administered to humans. The attenuated rVSV tested in this study was shown to be well tolerated at high doses in the highly sensitive mouse model by all three routes of inoculation whereas the more virulent prototypic VSV induced significant illness following IN or IV inoculation. Both the attenuated and prototypic viruses showed minimal dissemination following IM inoculation, supporting the selection of this route for future first-in-man clinical trials with rVSV vectors. In addition, the attenuated rVSV did not exhibit any adverse clinical signs such as weight loss, paralysis or death despite its widespread tissue distribution in the IV and IN studies. Consistent with its attenuated phenotype in vitro, the N4CT9-Gag1 virus did not replicate as vigorously in vivo as the prototypic Gag5 virus, which was underscored by the statistical significance of the reduced viral loads in the majority of tissues for the N4CT9-Gag1 groups as compared to the Gag5 groups at the majority of time points.

Furthermore, despite the significantly reduced replication levels of the attenuated virus compared to the prototype, the anti-Gag immune responses in mice inoculated IM with the attenuated virus were equal to or greater than those responses induced with the prototypic vector [34]. This robust immunogenicity associated with the use of the attenuated vector may be due to enhanced expression of the Gag gene by nature of its promoter-proximal position within the modified genome (Gag1), as compared to the prototypic vector, in which the Gag gene is more distal to the genomic promoter (Gag5). Indeed, this notion is supported in these studies by comparing the Gag mRNA levels to the gRNA levels between the two vectors. For all three routes of inoculation, the gRNA levels of the attenuated vector were significantly lower than the corresponding gRNA levels of the prototypic vector in more tissues and at more time points than was observed for the corresponding Gag mRNA levels (compare the number of statistically significant differences in panels D and F in Figs. 1–3).

The restricted spread of VSV following IM inoculation in adult mice, originally described by Sabin and Olitsky [41], was similar to what was recently reported for infection in cattle, a natural host [44]. In the bovine study, viral spread was limited to the inoculation site and draining lymph nodes in a similar manner to what was seen with IM inoculation in mice in this study. This limited spread in cattle by an experimental model of natural infection may explain why cattle naturally infected with VSV do not develop neurological disease. Similarly, wt VSV_{NJ} demonstrated restricted ability to spread to neuronal tissue following intradermal inoculation of adult deer mice; this restriction was absent from juvenile deer mice, however [14]. In the murine studies described herein, neither the attenuated virus nor the more virulent prototypic virus yielded adverse neurological findings or evidence of neuroinvasion after IM inoculation. Sabin and Olitsky proposed that there are natural barriers to the spread of VSV in adult mice that keep VSV from entering neuronal tissue following IM inoculation [41], an idea supported by the present studies.

Interestingly, while VSV infection was detected in brains of animals infected IV with either attenuated or prototypic virus, there was minimal (Gag5) or no (N4CT9) detectable neuropathology observed in the brains, despite the kinetics of infection indicating active replication (peaking at days 2–4) in the brain. Moreover, the level of Gag5 detected in the brain was well above the doses required to induce lethal encephalitis following direct intracranial (IC) inoculation, as the IC LD_{50} for Gag5 is less than 5 PFU [25]. Studies utilizing VSV vectors expressing GFP are being pursued to determine the cellular localization of VSV infection in the brain and other organs following IV inoculation.

VSV administered by the IN route of inoculation is pathogenic in mice, especially in young mice. Juvenile mice succumb to a lethal encephalitis following transmission of VSV from the olfactory epithelium to the olfactory bulb via the olfactory nerve [14,45–49]. The results reported herein demonstrated that IN inoculation with the more virulent prototypic virus induced more weight loss and clinical signs of disease than was observed during systemic infection following IV inoculation. Following IN inoculation, Gag5 viral loads peaked at day 2 in brain. Since whole brain homogenates were used for virus analysis in this study, it is possible that the infectious virus or viral RNA may have been concentrated in the olfactory bulb region of the brain. The peak virus titer of $\sim 10^6$ PFU/10 mg of tissue seen in brain homogenates of animals receiving prototypic rVSV by the IN route was $>10^5$ times higher than the IC LD_{50}, yet the mice showed limited morbidity and minimal neuropathology. It is possible that more severe neuropathology occurred in the subset of mice that died following IN inoculation with the prototypic vector, but we were unable to assess their brains for viral loads or histopathology. In contrast, mice receiving attenuated rVSV intranasally exhibited significantly lower levels of infectious virus in brain and exhibited no signs of morbidity or mortality. Furthermore, there was less systemic spread of virus following IN instillation of the attenuated virus as well as no detectable viremia. These findings with N4CT9-Gag1 are in agreement with analysis of related attenuated VSV vectors that showed that compared to the wt vector, a truncated cytoplasmic tail VSV vector (rVSV-CT1) spread significantly less to the lymph nodes and other organs when inoculated by the IN route [50].

A few previous studies have addressed persistence of VSV following infection in cattle, its natural host [51] and in experimental rodent models [50–53]. In order to understand the nature of VSV persistence in animals following infection and convalescence,

Letchworth and colleagues experimentally infected hamsters and cattle with VSV NJ serotype [51,52]. While viral genomic RNA determined by specific RT-PCR persisted in brain, liver, spleen, kidney, and lung tissues of animals for several months following infection, no infectious virus was recovered from these tissues. In the studies described herein, the highly sensitive Q-PCR assays for viral RNA detected the presence of viral gRNA as well as of mRNA from both viruses in animal tissues long after clearance of infectious viruses. Among the tissues, lymph nodes were the major sites of persistence of VSV genomes, especially following IN inoculation. A recent study in mice showed that compared to the wt vector, attenuated (rVSV-CT1) or single-cycle VSV (rVSVΔG) vectors spread and persisted significantly less following IN inoculation, and this reduced spread and persistence correlated with a reduction in immune responses by this route [50]. Nonetheless, these vectors showed persistence of genomic RNA in lymph nodes after clearance of infectious virus. To explain the persistence of viral gRNA in lymph nodes, Rose and co-workers [50] suggested two possible models: low level long-term viral replication, or the persistence of RNA contained within nucleocapsids that are cleared slowly. In addition, a recent study reported persistence of VSV encoded antigen in lymph nodes 6 weeks after IN inoculation [53], and the authors suggested that persistent nucleocapsids were undergoing low levels of transcription and translation, resulting in antigen expression. Our data support the model of persistent nucleocapsids that may undergo low levels of transcription, because we were able to detect gRNA, and in some cases Gag mRNA, in tissues, particularly lymph nodes, long after infectious virus had disappeared.

The attenuated rVSV vector, N4CT9-Gag1, was well tolerated and was non-pathogenic even during systemic infection, demonstrating the near absence of vector-associated pathogenicity of this attenuated construct in this highly permissive animal model. Furthermore, the localized dissemination of this virus delivered intramuscularly would suggest IM as the preferred route of administration for first-in-man evaluation. These findings will aid in the development and clinical evaluation of attenuated VSV vectors and suggest a possible mechanism for the enhanced immunogenicity [34] of attenuated rVSV vectors.

Acknowledgements

The authors wish to acknowledge Heather Arendt, Deborah Branch, Joanne DeStefano, and Min Guo for their assistance with the in vivo portions of the studies, Farooq Nasar and Irene Yurgelonis for assistance with viral stock preparation and viral load analysis, and Charles B. Clifford, DVM, PhD, DACVP, and Nancy Stedman, DVM, PhD, DACVP, for assistance with the histopathological analyses.

We also thank Susan Hoiseth for helpful comments on the manuscript.

This work was supported by NIH Contract N01-AI-25458.

References

[1] Rose JK, Whitt MA. Rhabdoviridae: the viruses and their replication. In: Knipe DM, Howley PM, Griffin DE, Lamb RA, Martin MA, Roizman B, et al., editors. Fields' virology. 4th edition Philadelphia: Lippincott Williams & Wilkins; 2001.
[2] Brandly CA, Hanson RP. Epizootiology of vesicular stomatitis. Am J Public Health 1957;47(2):205–9.
[3] Brody JA, Fischer GF, Peralta PH. Vesicular stomatitis virus in Panama. Human serologic patterns in a cattle raising area. Am J Epidemiol 1967;86(1):158–61.
[4] Fellowes ON, Dimopoullos GT, Callis JJ. Isolation of vesicular stomatitis virus from an infected laboratory worker. Am J Vet Res 1955;16(61 Part 1):623–6.
[5] Ferris DH, Hanson RP, Dicke RJ, Roberts RH. Experimental transmission of vesicular stomatitis virus by Diptera. J Infect Dis 1955;96(2):184–92.
[6] Fields BN, Hawkins K. Human infection with the virus of vesicular stomatitis during an epizootic. N Engl J Med 1967;277(19):989–94.
[7] Hanson RP, Rasmussen Jr AF, Brandly CA, Brown JW. Human infection with the virus of vesicular stomatitis. J Lab Clin Med 1950;36(5):754–8.
[8] Heiny E. Vesicular stomatitis in cattle and horses in Colorado. North Am Veterinarian 1945;26:726–30.
[9] Johnson KM, Vogel JE, Peralta PH. Clinical and serological response to laboratory-acquired human infection by Indiana type vesicular stomatitis virus (VSV). Am J Trop Med Hyg 1966;15(2):244–6.
[10] Reif JS, Webb PA, Monath TP, Emerson JK, Poland JD, Kemp GE, et al. Epizootic vesicular stomatitis in Colorado 1982 infection in occupational risk groups. Am J Trop Med Hyg 1987;36(1):177–82.
[11] Webb PA, Monath TP, Reif JS, Smith GC, Kemp GE, Lazuick JS, et al. Epizootic vesicular stomatitis in Colorado 1982 epidemiologic studies along the northern Colorado front range. Am J Trop Med Hyg 1987;36(1):183–8.
[12] Bruno-Lobo M, Peralta PH, Bruno-Lobo GG, de Paola D. Pathogenesis of vesicular stomatitis virus New Jersey infection in the adult hamster and mouse. Ann Microbiol (Rio J) 1968;15:69–80.
[13] Bruno-Lobo M, Peralta PH, Bruno-Lobo GG, de Paola D. Pathogenesis of vesicular stomatitis virus infection in the infant hamster and mouse. Ann Microbiol (Rio J) 1968;15:53–68.
[14] Cornish TE, Stallknecht DE, Brown CC, Seal BS, Howerth EW. Pathogenesis of experimental vesicular stomatitis virus (New Jersey serotype) infection in the deer mouse (*Peromyscus maniculatus*). Vet Pathol 2001;38(4):396–406.
[15] Flanagan EB, Schoeb TR, Wertz GW. Vesicular stomatitis viruses with rearranged genomes have altered invasiveness and neuropathogenesis in mice. J Virol 2003;77(10):5740–8.
[16] Forger 3rd JM, Bronson RT, Huang AS, Reiss CS. Murine infection by vesicular stomatitis virus: initial characterization of the H-2d system. J Virol 1991;65(9):4950–8.
[17] Huneycutt BS, Bi Z, Aoki CJ, Reiss CS. Central neuropathogenesis of vesicular stomatitis virus infection of immunodeficient mice. J Virol 1993;67(11):6698–706.
[18] Rabinowitz SG, Johnson TC, Dal Canto MC. The uncoupled relationship between the temperature-sensitivity and neurovirulence in mice of mutants of vesicular stomatitis virus. J Gen Virol 1977;35(2):237–49.
[19] Wagner RR. Pathogenicity and immunogenicity for mice of temperature-sensitive mutants of vesicular stomatitis virus. Infect Immun 1974;10(2):309–15.
[20] Youngner JS, Wertz G. Interferon production in mice by vesicular stomatitis virus. J Virol 1968;2(11):1360–1.
[21] Clarke DK, Cooper D, Egan MA, Hendry RM, Parks CL, Udem SA. Recombinant vesicular stomatitis virus as an HIV-1 vaccine vector. Springer Semin Immunopathol 2006;28(3):239–53.
[22] Majid AM, Ezelle H, Shah S, Barber GN. Evaluating replication-defective vesicular stomatitis virus as a vaccine vehicle. J Virol 2006;80(14):6993–7008.
[23] Roberts A, Kretzschmar E, Perkins AS, Forman J, Price R, Buonocore L, et al. Vaccination with a recombinant vesicular stomatitis virus expressing an influenza virus hemagglutinin provides complete protection from influenza virus challenge. J Virol 1998;72(6):4704–11.
[24] Johnson JE, Nasar F, Coleman JW, Price RE, Javadian A, Draper K, et al. Neurovirulence properties of recombinant vesicular stomatitis virus vectors in non-human primates. Virology 2007;360(1):36–49.
[25] Clarke DK, Nasar F, Lee M, Johnson JE, Wright K, Calderon P, et al. Synergistic attenuation of vesicular stomatitis virus by combination of specific G gene truncations and N gene translocations. J Virol 2007;81(4):2056–64.
[26] Schnell MJ, Buonocore L, Boritz E, Ghosh HP, Chernish R, Rose JK. Requirement for a non-specific glycoprotein cytoplasmic domain sequence to drive efficient budding of vesicular stomatitis virus. EMBO J 1998;17(5):1289–96.
[27] Wertz GW, Perepelitsa VP, Ball LA. Proceedings of the National Gene rearrangement attenuates expression and lethality of a nonsegmented negative strand RNA virus. Proc Natl Acad Sci USA 1998;95(7):3501–6.
[28] Abraham G, Banerjee AK. Sequential transcription of the genes of vesicular stomatitis virus. Proc Natl Acad Sci USA 1976;73(5):1504–8.
[29] Ball LA, White CN. Order of transcription of genes of vesicular stomatitis virus. Proc Natl Acad Sci USA 1976;73(2):442–6.
[30] Davis NL, Wertz GW. Synthesis of vesicular stomatitis virus negative-strand RNA in vitro: dependence on viral protein synthesis. J Virol 1982;41(3):821–32.
[31] Emerson SU, Yu Y. Both NS and L proteins are required for in vitro RNA synthesis by vesicular stomatitis virus. J Virol 1975;15(6):1348–56.
[32] Iverson LE, Rose JK. Localized attenuation and discontinuous synthesis during vesicular stomatitis virus transcription. Cell 1981;23(2):477–84.
[33] Villarreal LP, Breindl M, Holland JJ. Determination of molar ratios of vesicular stomatitis virus induced RNA species in BHK21 cells. Biochemistry 1976;15(8):1663–7.
[34] Cooper D, Wright KJ, Calderon PC, Guo M, Nasar F, Johnson JE, et al. Attenuation of recombinant vesicular stomatitis virus HIV-1 vaccine vectors by gene translocations and G gene truncation reduces neurovirulence and enhances immunogenicity in mice. J Virol 2008;82(1):207–19.
[35] Pan D, Gunther R, Duan W, Wendell S, Kaemmerer W, Kafri T, et al. Biodistribution and toxicity studies of VSVG-pseudotyped lentiviral vector after intravenous administration in mice with the observation of in vivo transduction of bone marrow. Mol Ther 2002;6(1):19–29.
[36] Coleman JW, Ogin-Wilson E, Johnson JE, Nasar F, Zamb TP, Clarke DK, et al. Quantitative multiplex assay for simultaneous detection of the Indiana serotype of vesicular stomatitis virus and HIV gag. J Virol Methods 2007;143(1):55–64.
[37] Lefrancois L, Lyles DS. The interaction of antibody with the major surface glycoprotein of vesicular stomatitis virus. II. Monoclonal antibodies of non-neutralizing and cross-reactive epitopes of Indiana and New Jersey serotypes. Virology 1982;121(1):168–74.
[38] Olitsky PK, Cox HR, Syverton JT. Comparative studies on the viruses of vesicular stomatitis and equine encephalomyelitis. J Exp Med 1934;59(2):159–71.

[39] Olitsky PK, Sabin AB, Cox HR. An acquired resistance of growing animals to certain neurotropic viruses in the absence of humoral antibodies or previous exposure to infection. J Exp Med 1936;64(5):723–37.
[40] Sabin AB, Olitsky PK. Influence of host factors on neuroinvasiveness of vesicular stomatitis virus: I. Effect of age on the invasion of the brain by virus instilled in the nose. J Exp Med 1937;66(1):15–34.
[41] Sabin AB, Olitsky PK. Influence of host factors on neuroinvasiveness of vesicular stomatitis virus: II. Effect of age on the invasion of the peripheral and central nervous systems by virus injected into the leg muscles or the eye. J Exp Med 1937;66(1):35–57.
[42] Sabin AB, Olitsky PK. Influence of host factors on neuroinvasiveness of vesicular stomatitis virus: III. Effect of age and pathway of infection on the character and localization of lesions in the central nervous system. J Exp Med 1938;67(2):201–28.
[43] Sabin AB, Olitsky PK. Influence of host factors on neuroinvasiveness of vesicular stomatitis virus: IV. Variations in neuroinvasiveness in different species. J Exp Med 1938;67(2):229–49.
[44] Scherer CF, O'Donnell V, Golde WT, Gregg D, Mark Estes D, Rodriguez LL. Vesicular stomatitis New Jersey virus (VSNJV) infects keratinocytes and is restricted to lesion sites and local lymph nodes in the bovine, a natural host. Vet Res 2007;38(3):375–90.
[45] Lundh B, Kristensson K, Norrby E. Selective infections of olfactory and respiratory epithelium by vesicular stomatitis and Sendai viruses. Neuropathol Appl Neurobiol 1987;13(2):111–22.
[46] Huneycutt BS, Plakhov IV, Shusterman Z, Bartido SM, Huang A, Reiss CS, et al. Distribution of vesicular stomatitis virus proteins in the brains of BALB/c mice following intranasal inoculation: an immunohistochemical analysis. Brain Res 1994;635(1–2):81–95.
[47] Plakhov IV, Arlund EE, Aoki C, Reiss CS. The earliest events in vesicular stomatitis virus infection of the murine olfactory neuroepithelium and entry of the central nervous system. Virology 1995;209(1):257–62.
[48] Reiss CS, Plakhov IV, Komatsu T. Viral replication in olfactory receptor neurons and entry into the olfactory bulb and brain. Ann NY Acad Sci 1998;855:751–61.
[49] van den Pol AN, Dalton KP, Rose JK. Relative neurotropism of a recombinant rhabdovirus expressing a green fluorescent envelope glycoprotein. J Virol 2002;76(3):1309–27.
[50] Simon ID, Publicover J, Rose JK. Replication and propagation of attenuated vesicular stomatitis virus vectors in vivo: vector spread correlates with induction of immune responses and persistence of genomic RNA. J Virol 2007;81(4):2078–82.
[51] Letchworth GJ, Barrera JC, Fishel JR, Rodriguez L. Vesicular stomatitis New Jersey virus RNA persists in cattle following convalescence. Virology 1996;219(2):480–4.
[52] Barrera JC, Letchworth GJ. Persistence of vesicular stomatitis virus New Jersey RNA in convalescent hamsters. Virology 1996;219(2):453–64.
[53] Turner DL, Cauley LS, Khanna KM, Lefrancois L. Persistent antigen presentation after acute vesicular stomatitis virus infection. J Virol 2007;81(4):2039–46.